JOURNAL OF MATERIALS SCIENCE 30 (1995) 3075–3081

Thermal stability improvement on pore and phase structure of sol–gel derived zirconia

R. GOPALAN, C.-H. CHANG, Y.S. LIN*
Department of Chemical Engineering, University of Cincinnati, Cincinnati, OH 45221, USA

Thermal stability improvement of mesoporous zirconia is important for its applications as catalyst supports or membrane layers at high temperatures. Yttria-coated zirconia is synthesized by doping a small amount of yttrium nitrate solution in zirconia sol. The sol–gel derived undoped and 2 and 3 mol% yttria-doped zirconia samples after calcination at 450 °C are in the metastable phase. Undoped zirconia starts to transform to thermodynamically stable monoclinic phase at 600 °C. The yttria-doped zirconia samples remain in the metastable phase after heat treatment in air at 900 °C for 30 h. Doping yttria also retards the sintering and grain-growth rates of the sol–gel derived zirconia. Doping with 2 mol% yttria gives the most effective results with respect to retarding the surface area loss of zirconia at high temperature. Yttria with a loading up to 2 mol % is possibly present on the grain surface of zirconia. The improvement of the thermal stability of zirconia by coating yttria is explained in terms of the effects of dopant on the mobility and concentration of the surface defects.

1. Introduction

Porous zirconia is attracting increasing interest on account of its use as a catalyst support or membrane [1, 2] partly because it is chemically more stable than the classic materials such as γ-alumina and silica. Nanostructured zirconia prepared by several chemical methods (e.g. co-precipitation method, sol–gel method) is usually in a metastable phase (e.g. tetragonal phase) [1–4]. At a temperature of about 600 °C, zirconia starts to transform from the metastable (tetragonal) phase to the stable monoclinic phase [3]. This phase transformation is accompanied by a dramatic change in pore structure of zirconia. At temperatures lower than the phase transformation temperature, the pore structure of zirconia also changes, but to a lesser extent, as a result of sintering and grain growth. For high-temperature applications, the structure stability of nanostructured zirconia should be improved.

To stabilize the tetragonal phase of zirconia, Shi *et al.* [4] doped yttria, ceria or magnesia in zirconia. Mercera *et al.* [5] recently reported doping yttria or lanthana in zirconia. In both studies the doped zirconia was synthesized by the co-precipitation method which gives a solid solution of zirconia and dopant. They found doping reduces the sintering and grain-growth rates. Doping yttria or lanthana substantially stabilizes the tetragonal phase of zirconia. They proposed that doping reduces the sintering and grain-growth rate by either lowering the surface energy of the zirconia grain [4] or decreasing the concentration of mobile species on the grain surface [5]. Nevertheless, the exact mechanism on retarding the phase transformation is not clear.

Another approach reported for retarding the metastable to stable phase transformation of a ceramic material is to coat a second oxide on the ceramic grain surface in order to reduce the nucleation sites on the grain boundary and/or to increase the nucleation activation energy [6, 7]. Coating a second oxide could also reduce the sintering rate. This approach was more often employed to improve the thermal stability of γ-alumina [7–10]. This coating method was also extensively used to coat a catalytic active species (salt or oxide) on catalyst supports, such as MoO_3, $CuCl_2$, V_2O_3, La_2O_3 on γ-alumina or silica [11].

The coating method is, in principle, very different from the co-precipitation method which results in a solid solution. Coating a second oxide or a salt on the surface of solid oxide is often accomplished with the wet-impregnation and thermal-dispersion methods [11]. In these coating processes, the solid oxide particles are brought into contact with liquid solution or solid containing the dopant. Xie and Tang [11] believed that the dopant coated by these methods was present as a monolayer or sub-monolayer on the grain surface of the support. They theorized that the formation of a monolayer of a dopant on the surface of the support is a thermodynamically favourable process if the dopant, with a metal ion size larger than the size of the metal ion of the ceramic oxide, can form a strong surface bond with the oxide particles. Several other investigators [8, 9, 12] also suggested that dopant is present as a two-dimensional layer covering the grain surface of the ceramic oxide.

The sol–gel method has been used to fabricate mesoporous and microporous zirconia membranes

---

* Author to whom all correspondence should be addressed.

0022–2461

[3, 13]. Mesoporous zirconia catalyst supports with a uniform pore-size distribution, large surface area and excellent mechanical strength can also be prepared by the sol–gel method. Lin *et al.* [14] recently reported an effective method (referred to here as the solution–sol mixing method) for improving the thermal stability of the sol–gel derived alumina, titania and zirconia. In this method, a small amount of lanthanum or yttrium nitrate solution was doped into boehmite, titania or zirconia sol. The thermal stability of the resulting alumina, titania and zirconia was substantially improved.

The solution–sol mixing method is more efficient compared to the conventional wet-impregnation coating method because it avoids several additional steps required in the conventional doping method. Furthermore, this method allows precise control of the amount of dopant. The objective of the present work was to demonstrate further the use of this method for thermal stability improvement on the pore and phase structure of sol–gel derived zirconia at high temperatures.

2. Materials and methods

Stable 0.25 M zirconia sol was prepared by hydrolysis and condensation of zirconium *n*-propoxide in a water/propanol solution. In synthesis, 123 ml zirconium *n*-propoxide (Alfa) was diluted with 500 ml isopropanol and 900 ml water in a nitrogen glove box. The resulting zirconia precipitates were washed with water and filtered to remove the alcohol. The zirconia precipitates were then diluted in 1 l of water and peptized with 125 ml 1 M HNO_3 at 90–100 °C under refluxing conditions. The stable zirconia sol was mixed with poly(vinyl alcohol) (PVA) and hydroxy propyl cellulose solutions which serve as the binder for the drying step. 20 $g\,l^{-1}$ yttrium nitrate solution was prepared by mixing 2 g yttrium nitrate with 95 ml water and 5 ml 1 M nitric acid.

A fixed amount of yttrium nitrate solution, depending on the mole ratio of yttria to zirconia required, was added to the zirconia sol and the resulting sol was rapidly mixed. The extent of doping was limited by the stability of the resulting mixed sol. The maximum amount of yttria that could be doped into zirconia was 5 mol%. In doping the yttrium nitrate solution into the zirconia sol, the pH value of the mixed sol was kept close to that of the undoped sol, so that the doped sol was still stable.

Undoped and yttria-doped zirconia samples were prepared by drying a given amount of corresponding sols in petri dishes at 40 °C and 40%–50% relative humidity. The dried xerogels were calcined in air in a temperature-programmable furnace at 450 °C for 3 h, with a heating and cooling rate of 0.5 $°C\,min^{-1}$. The yttrium nitrate was converted to yttria during the calcination. Some of the calcined zirconia samples were heat treated at 450, 600, 700 and 900 °C for 30 h in air.

The surface area, pore volume, pore size and pore-size distribution of the zirconia samples were obtained from nitrogen ad(de)sorption isotherms using an adsorption porosimeter (Micrometrics, ASAP 2000). The phase structures of the samples were identified by X-ray diffractometer (Siemens, Cu$K_{\alpha1}$). Crystal size was calculated from X-ray diffraction (XRD) data using Scherrer's method [15]. The yttria composition of heat-treated samples was also measured by energy dispersive spectroscopy (EDS) (Cambridge Scanning Electron Microscope 90B). Powdered samples were used in both the XRD and energy dispersive X-ray analysis (EDX) measurements.

3. Results and discussion

Table I summarizes the pore size, surface area and pore volume of the undoped and yttria-doped zirconia samples after calcination at 450 °C for 3 h. The pore structure of the doped zirconia samples was not the same as the undoped zirconia. However, the difference observed in the pore structure between the undoped and doped zirconia samples is relatively minor. To examine whether the solution–sol mixing method is generally applicable for other systems, experiments were also performed to dope several other salt solutions into particulate boehmite (γ-AlOOH) and titania sols. The results are also summarized in Table I. Synthesis of the boehmite and titania sols was described in detail elsewhere [3]. Nitric acid was used to pepetize all the particulate sols summarized in Table I.

For most of the cases shown in Table I, the sols after doping still remained stable. The pore structures of the doped samples after calcination do not differ much from the corresponding undoped samples, as shown in Table I. However, mixing a dopant with a salt containing a different anion from that of the acid used in pepetization, destabilized the sols. The pore structure of the samples derived from the unstable sols is very different from those derived from the stable sols.

The pore structure of the samples after calcination is determined by the shape and size of the primary particles, and, to a lesser extent, by the manner in which these particles are packed. The slight differences in the pore structure between the undoped and doped samples are due to the effects of dopant on the primary particle size and shape in the sol. The particulate sols listed in Table I contain fine particles of zirconia, boehmite or titania. Mixing a salt solution in the sol might change slightly the cation charge distribution, affecting the particle size and shape of the primary particles. The following points were found to be critical in ensuring the stability of a sol after doping: (1) the preferred precursor for the dopant is the salt containing the same anion as that of the acid used in pepetization; (2) the pH of the doped sol should remain essentially the same as the undoped sol; (3) the sol should be rigorously mixed while the dopant solution is added into the sol.

The exact location of the dopant ions in the doped sol is not yet clear and requires further fundamental study on the solution–sol mixing method. However, it can be assumed that the doped salt is coated on the grain surface of the primary particles in the drying

TABLE I Comparison of pore structure of doped and undoped zirconia, alumina and titania synthesized by the solution–sol mixing method

Sol	Doping salt	Loading[a]	S_{BET} (m^2g^{-1})	V_p ($ml\,g^{-1}$)	d_{av} (nm)
ZrO_2	Pure	0	67	0.13	3·5
	$Y(NO_3)_3$	0.04	66	0.11	3·1
	$Y(NO_3)_3$	0.06	78	0.11	2·8
Boehmite	Pure	0	323	0.36	3·1
	$Ca(NO_3)_2$	0.20	298	0.25	2·9
	$Cu(NO_3)_2$	0.14	302	0.28	2·9
	$Ag(NO_3)$	0.10	262	0.25	2·8
	$La(NO_3)_3$	0.03	290	0.28	3·1
	$CuCl_2$	0.20	207	0.18	2·9[b]
TiO_2	Pure	0	177	0.31	5·0
	$La(NO_3)_3$	0.08	184	0.30	5·2
	$CuCl_2$	0.22	8	0.03	8·5[b]

[a] Mole ratio of dopant cation to the cation of sol (Zr, Al or Ti).

[b] Sol becomes unstable after mixing, with large aggregates precipitated.

TABLE II Loading of yttria in the zirconia samples

Sample	$Y_2O_3/(Y_2O_3+ZrO_2)$[a]		Measured by EDS	
	(wt %)	(mol %)	Atomic Y (%)	Y_2O_3 (mol %)
1	0.00	0.0	0.00	0.00
2	3.61	2.0	9.28	4.87
3	5.36	3.0	11.46	6.08

[a] Calculated from the amounts of salt solution and sol used in preparing each sample.

process. After calcination at 450 °C, the coated salt is converted to the corresponding oxide which may still remain on the grain surface of the primary particles.

The concentrations of yttria in zirconia calculated from the amounts of salt solution and sol used in preparing each sample, and those determined by EDS, are listed in Table II. The yttria percentages shown in the figures and the text are mole percentages calculated from the amounts of salt solution and sol. Figs 1 and 2 show the variation of the surface area and pore size of the zirconia samples with heat-treatment temperature. The surface area decreases and the pore size increases with increasing temperature. From these results, a correct comparison between the thermal stability of the undoped and yttria-doped zirconia samples cannot be made, because the initial surface area and the pore size also vary with dopant concentration. Nevertheless, the following conclusions can be drawn from these experimental results. The surface area decrease and the pore size increase are much more rapid for undoped zirconia compared to the 2 and 3 mol % yttria-doped membranes, due to the improved thermal stability of the doped samples.

To compare effectively the thermal stability of the undoped and yttria-doped samples, the surface area was corrected by expressing it as the change in surface area, while the pore size was corrected by dividing by the initial pore size. These results are plotted in Figs 3 and 4. From these figures it can be observed that doping has retarded surface-area change very effectively. The level of doping has an important effect on the surface area and pore-size variation. Doping with 2 mol % gives better surface area and pore-size

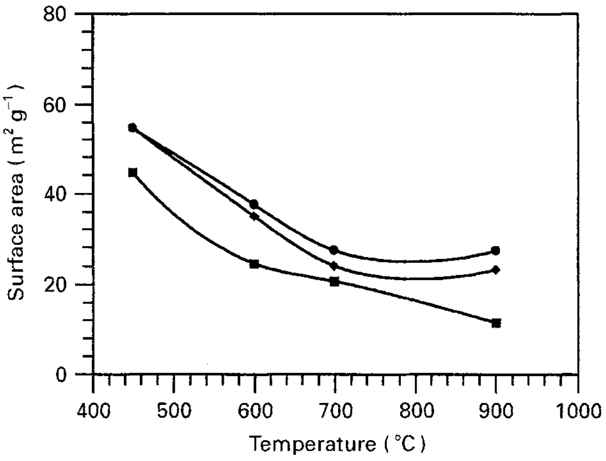

Figure 1 Variation of the surface area of (■) undoped and (●) 2 and (◆) 3 mol % yttria-doped zirconia samples with heat-treatment temperatures.

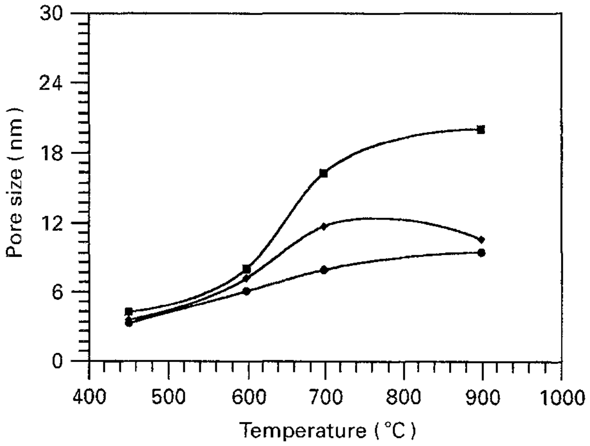

Figure 2 Variation of the pore size of (■) undoped and (●) 2 and (◆) 3 mol % yttria-doped zirconia samples with heat-treatment temperature.

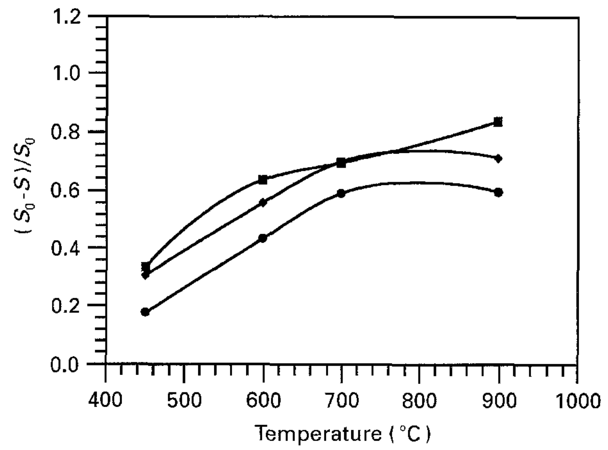

Figure 3 Variation of the change of surface area of (■) undoped and (●) 2 and (◆) 3 mol % yttria-doped zirconia samples with heat-treatment temperature.

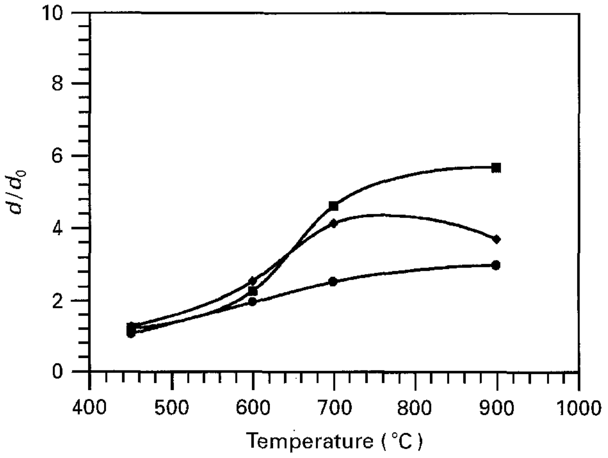

Figure 4 Variation of the relative pore size of (■) undoped and (●) 2 and (◆) 3 mol % yttria-doped zirconia samples with heat-treatment temperature.

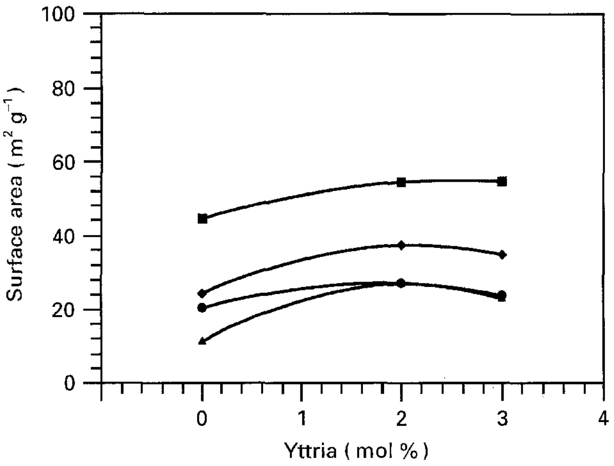

Figure 5 Variation of surface area of zirconia with dopant concentration at different heat-treatment temperatures: (■) 450 °C, (◆) 600 °C, (●) 700 °C, (▲) 900 °C.

stability than the undoped and 3 mol % yttria-doped zirconia. To observe the stability at different temperatures as a function of doping, the surface area and the change in surface area were plotted against the dopant concentration for different temperatures of heat treatment. These results are shown in Figs 5 and 6. This

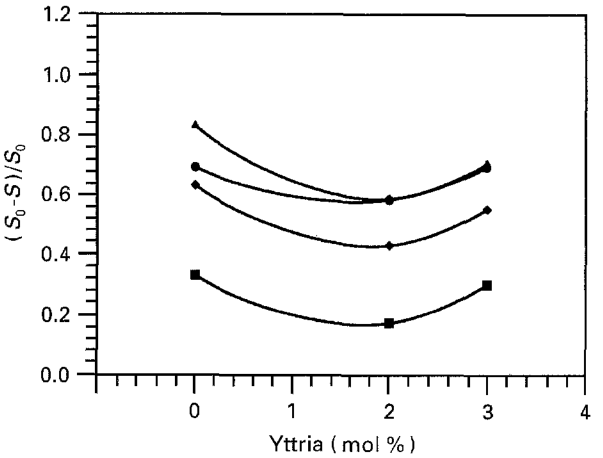

Figure 6 Variation of the change in surface area of zirconia membranes with dopant concentration at different heat-treatment temperatures: (■) 450 °C, (◆) 600 °C, (●) 700 °C, (▲) 900 °C.

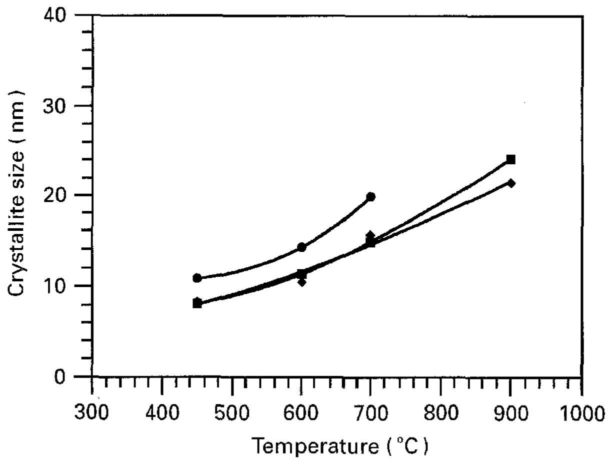

Figure 7 Variation of the crystallite size of (●) undoped and (■) 2 and (◆) 3 mol % yttria-doped zirconia samples (in metastable phase) with heat-treatment temperatures.

further shows the optimum effect of yttria on the thermal stability. There is an optimum in surface area change at 2 mol % doping, irrespective of the temperature of heat treatment.

Grain sizes calculated from the (tetragonal) zirconia (1 1 1) reflection are plotted in Fig. 7. Doping yttria has resulted in a smaller grain size compared to undoped zirconia, indicating the retarding effect of yttria on grain growth. Apart from this, the activation energy of grain-size variation seems to have increased, as seen from the flatter dependence of grain size on temperature for the yttria-doped zirconia samples compared to the undoped zirconia. The yttria content does not seem to have any consistent effect on the grain-growth retardation in the temperature range investigated.

As reported by Chang *et al.* [3], for the undoped zirconia in the low-temperature range of 40–600 °C, predominantly sintering and to some extent grain growth, and in the high-temperature range of 600–900 °C, grain growth and associated phase transformation, are the main mechanisms by which surface area decreases. At temperatures lower than 1000 °C, surface diffusion is the mechanism by which sintering and grain growth take place [17]. The sintering and grain-growth rate due to surface diffusion are dependent on the concentration and mobility of defects on the surface.

It is suggested that in zirconia the major defect responsible for sintering and grain growth is the zirconium vacancy formed by (using the Kröger–Vink notations) [1]

$$\mathrm{Zr}_{\mathrm{Zr}}^{\mathrm{x}} + 2\mathrm{O}_{\mathrm{O}}^{\mathrm{x}} \rightarrow \mathrm{ZrO}_{2}^{\mathrm{x}} + \mathrm{V}_{\mathrm{Zr}}^{''''} + 2\mathrm{V}_{\mathrm{O}}^{\cdot\cdot} \qquad (1)$$

where $\mathrm{Zr}_{\mathrm{Zr}}^{\mathrm{x}}$ denotes a zirconium cation on a zirconium lattice site, $\mathrm{O}_{\mathrm{O}}^{\mathrm{x}}$ denotes an oxygen anion on an oxygen lattice site, $\mathrm{V}_{\mathrm{Zr}}^{''''}$ denotes a four-fold (negatively) charged zirconium vacancy and $\mathrm{V}_{\mathrm{O}}^{\cdot\cdot}$ denotes a doubly (positively) charged oxygen vacancy. The diffusional mass-transport flux is proportional to the product of diffusivity and concentration of the zirconium vacancy as

$$J \propto D[\mathrm{V}_{\mathrm{Zr}}^{''''}] \qquad (2)$$

When yttria is doped into zirconia, this yttria may form a two-dimensional layer on the surface of the zirconia particles. This reduces the mobility of the zirconium vacancy. As a result of this, sintering and crystal-growth rates decrease. Thus yttria coated on zirconia stabilizes the surface area and the zirconia grain. The results here indeed indicate that doping of yttria has retarded sintering and grain growth, as observed by the reduced surface-area change and lower grain size of yttria-doped zirconia. If the above discussed line of reasoning is followed, increasing the yttria doping should increase the surface coverage and decrease diffusivity of the zirconium vacancy and thus should result in decreased sintering rate or better stability. But the results of the surface area change as discussed before (Figs 5 and 6), indicate a clear optimum at 2 mol% yttria doping at all temperatures.

To examine the possibility of errors in controlling the amount of yttrium doped into the zirconia sol while synthesizing the samples, the samples heat treated at 600 °C were characterized by EDS. The concentration of yttria measured by EDS is also shown in Table II. The yttria concentrations measured by EDS do not match exactly the values of 2 and 3 mol% calculated in synthesis due to systematic errors of the EDS measurements. However, the yttria concentration in the 2 mol% doped sample measured by EDS is lower than that measured in the 3 mol% doped sample. This confirms that the 3 mol% sample indeed contains more yttria than the 2 mol% sample.

As discussed earlier, the doped yttria, present most likely on the grain surface of zirconia, could reduce the mobility of the mobile species (zirconium vacancy). This lowers the sintering and crystal-growth rates for the zirconia. The amount of yttria corresponding to the monolayer coverage is 0.19 g per 100 m^2 grain surface, calculated using the method suggested by Xie and Yang [11]. The yttria loadings in the samples summarized in Table II (0.055 and 0.068 g/100 m^2) are much smaller than the monolayer loading. Because Y^{3+} is not larger than Zr^{4+}, the doped yttria may not remain on the grain surface of zirconia up to the monolayer coating. At a concentration higher than 2 mol%, the doped $\mathrm{Y}_2\mathrm{O}_3$ may react with the oxygen vacancy on the grain surface as

$$\mathrm{YO}_{1.5} + 1.5\mathrm{V}_{\mathrm{O}}^{\cdot\cdot} \rightarrow \mathrm{Y}_{\mathrm{i}}^{\cdot\cdot\cdot\cdot\cdot} + 1.5\mathrm{O}_{\mathrm{O}}^{\mathrm{x}} \qquad (3)$$

Therefore, Reaction (3) consumes oxygen vacancies, shifting the equilibrium of Reaction (1) towards the right, which increases the zirconium vacancy concentration. Thus, the net effect is an increase in mass transport flux as described by Equation 2, though the mobility of the zirconium vacancy might be reduced. This might explain the optimum effect of doping 2 mol% yttria in stabilizing the surface-area reduction.

Figs 8–10 show the XRD data for the undoped, 2 and 3 mol% yttria-doped zirconia samples after heat treatment at different temperatures. The XRD data for undoped zirconia show a tetragonal-like phase after heat treatment at 450 °C. The phase structure of the undoped, 2 and 3 mol% yttria-doped zirconia after heat treatment at 450 °C are the same. Doping yttria into zirconia does not seem to affect the phase structure after calcination. Furthermore, no other XRD peaks such as those for crystalline $\mathrm{Y}_2\mathrm{O}_3$ are observed in the samples calcined at 450 °C. This suggests that $\mathrm{Y}_2\mathrm{O}_3$ is present in a form which is XRD undetectable.

It should be pointed out that cubic and tetragonal phases of zirconia are difficult to distinguish from the XRD patterns. Nevertheless, several studies [1, 2, 5] have shown that zirconia prepared by the wet-chemical methods with a grain size in the range 10–30 nm,

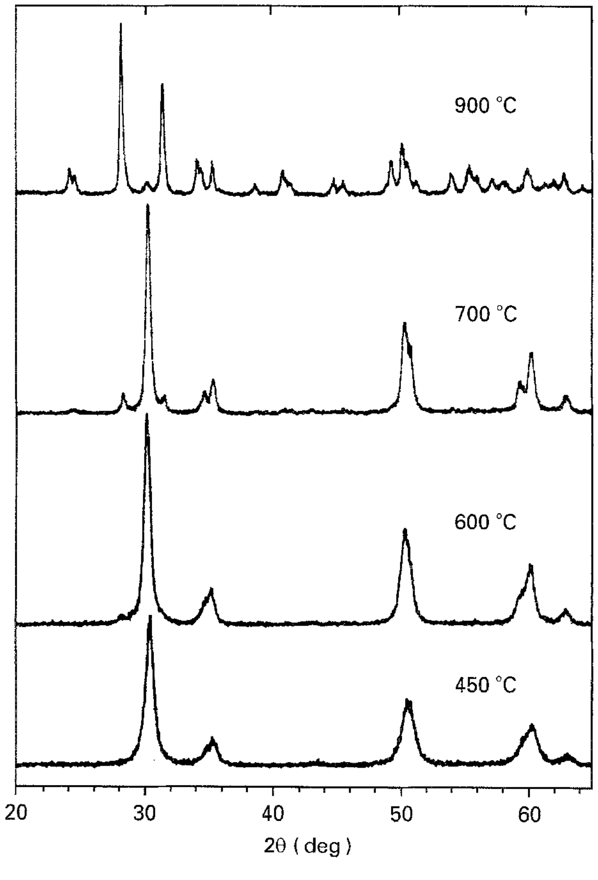

Figure 8 XRD peaks of undoped zirconia for different heat-treatment temperatures.

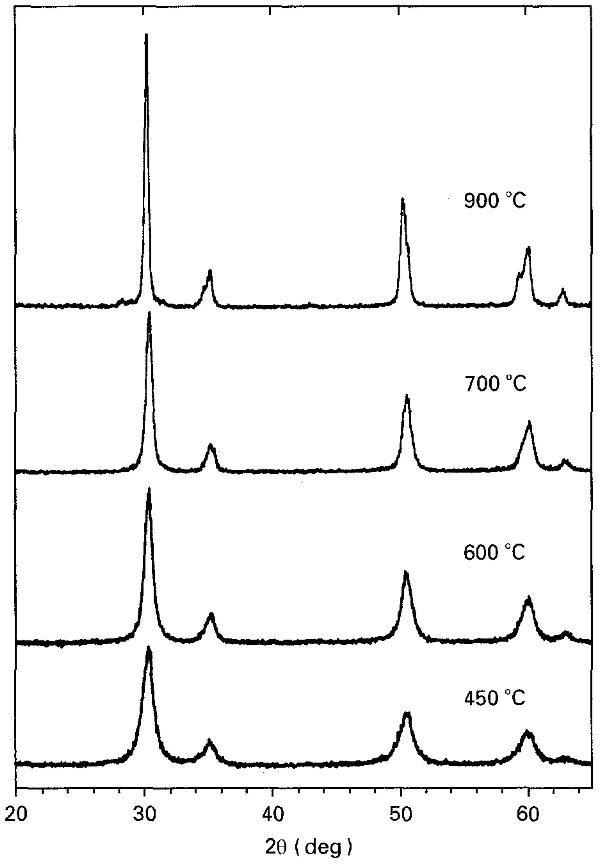

Figure 9 XRD peaks of 2 mol % yttria-doped zirconia for different heat-treatment temperatures.

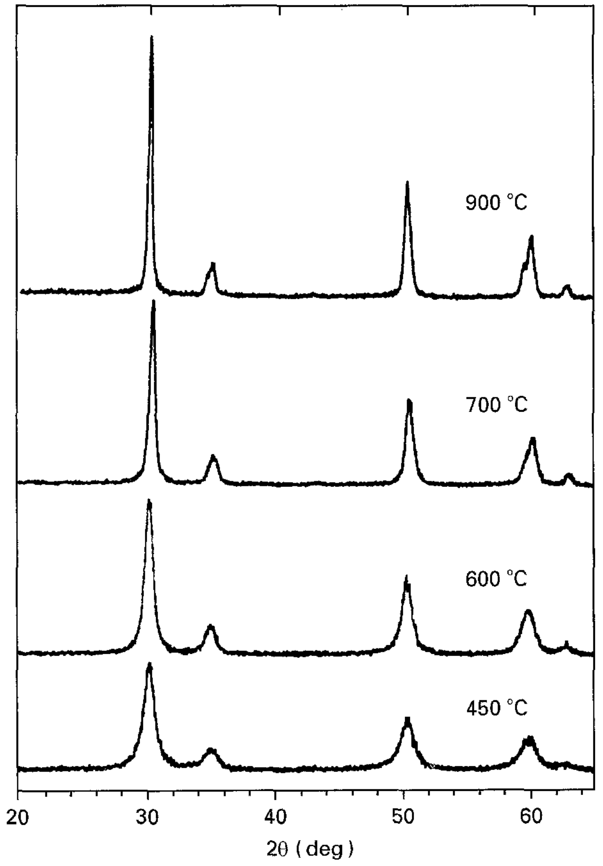

Figure 10 XRD peaks of 3 mol % of yttria-doped zirconia for different heat-treatment temperatures.

is in the tetragonal phase instead of the cubic phase. For the yttria-doped zirconia, such a low amount of yttria ($\leq$ 3 mol %) would unlikely result in stabilized cubic-phase zirconia. Therefore, the undoped, 2 and 3 mol% yttria-doped zirconia samples after calcination at 450 °C are also considered to be in the tetragonal phase, instead of the cubic phase.

For undoped zirconia, heat treatment at higher temperatures results in the tetragonal to monoclinic phase transformation. This phase transformation starts at 600 °C and is nearly complete at 900 °C. For the 2 and 3 mol % yttria-doped zirconia samples, heat treatment at higher temperatures does not result in the expected tetragonal to monoclinic phase transformation. No trace of the monoclinic phase is found in the yttria-doped zirconia samples even after heat treatment at 900 °C. Doping yttria in zirconia raises the phase transformation temperature by at least 300 °C.

The stable phase of zirconia in the temperature region in which the heat treatments were performed is monoclinic phase. But the sol–gel method produces the metastable phase of zirconia. This is because of the lower surface energy of the metastable phase (tetragonal or cubic) zirconia. Thus when zirconia grains are lower than a critical size, the tetragonal or cubic phase is stable. For tetragonal phase this critical size is about 30 nm when the elastic energy is considered and 10 nm when it is not [4, 18]. This critical size could increase when yttria is coated on zirconia because of change in the surface energy. On the other hand, addition of yttria lowers the grain-growth rate, as discussed before. Thus, the temperature or time required for the grains to reach a critical size is higher or longer for the yttria-doped zirconia samples.

4. Conclusion

Undoped and yttria-doped zirconia samples were prepared by the solution–sol method. There were very minor differences in the pore structure between the undoped and the yttria-doped zirconia samples. The minor differences in pore structure were attributed to the mixing of the salt solution with the sol, which altered the surface charge distribution and hence the primary particle size.

Doping with yttria stabilized the pore and phase structure of the sol–gel derived zirconia. The extent of stabilization was a strong function of the dopant content. The stabilization of the pore structure was due to the retardation of the sintering and grain-growth rates. Sintering and grain-growth rates were reduced because of the lower surface energy and diffusion coefficient. 2 mol % yttria doping resulted in a better stability compared to 3 mol % yttria-doped zirconia.

Doping with 2 or 3 mol % yttria completely retarded the metastable to monoclinic phase transformation up to 900 °C due to the decreased grain-growth rate and possibly an increase in the critical grain size required for transformation to occur.

Acknowledgement

This research was partially supported by the National Science Foundation (CTS-9209518).

References

1. P. D. L. MERCERA, V. J. G. OMMEN, E. B. M. DOESBURG, A. J. BURGGRAAF and J. R. H. ROOS, *Appl. Catal.* **57** (1990) 127.
2. A. LARBOT, J.-P. FABRE, C. GUIZARD and L. COT, *J. Am. Ceram. Soc.* **72** (1989) 257.
3. C.-H. CHANG, R. GOPALAN and Y. S. LIN, *J. Membrane Sci.* **91** (1994) 27.
4. J. L. SHI, Z. X. LIN and T. S. YEN, *J. Europ. Ceram. Soc.* **8** (1991) 117.
5. P. D. L. MERCERA, V. J. G. OMMEN, E. B. M. DOESBURG, A. J. BURGGRAAF and J. R. H. ROOS, *Appl. Catal.* **78** (1991) 79.
6. S. HISHITA, I. MUTOH, K. KUOMOTO and H. YANAGIDA, *Ceram. Int.* **61** (1983).
7. H. SCHAPER, E. B. M. DOESBURG, P. H. M. DE KORTE and L. L. VAN REIJEN, *Solid State Ionics* **16** (1985) 261.
8. M. BETTMAN, R. E. CHASE, K. OTTO and W. H. WEBER, *J. Catal.* **117** (1989) 447.
9. I. I. M. TIJBURG, J. W. GEUS and H. W. ZANDBERGEN, *J. Mater. Sci.* **26** (1991) 6479.
10. Y. S. LIN, K. J. DE VRIES and A. J. BURGGRAAF, *J. Mater. Sci.* **26** (1991) 715.
11. Y.-C. XIE and Y.-Q. TANG, *Adv. Catal.* **37** (1990) 1.
12. J. M. J. G. LIPSCH and G. C. A. SCHUIT, *J. Catal.* **15** (1969) 174.
13. Q. XU and M. A. ANDERSON, *J. Am. Ceram. Soc.* **76** (1993) 2093.
14. Y. S. LIN, C.-H. CHANG and R. GOPALAN, *Ind. Eng. Chem. Res.* **33** (1993) 860.
15. R. P. INGEL and D. LEWIS III, *J. Am. Ceram. Soc.* **69** (1986) 325.
16. H. P. K. KLUG and L. E. ALEXANDER, "X-Ray Diffraction Procedures" (Wiley, New York, 1954).
17. M. M. R. BOUTZ, G. S. A. M. THEUNISSEN, A. J. A. WINNUBST and A. J. BURGGRAAF, *Mater. Res. Soc. Symp. Proc.* **196** (1990) 87.
18. R. C. GARVIE, *J. Phys. Chem.* **82** (1978) 218.

Received 16 August 1994
and accepted 9 January 1995